Targeted Expression of IL-11 in the Murine Airway Causes Lymphocytic Inflammation, Bronchial Remodeling, and Airways Obstruction

Weiliang Tang,* Gregory P. Geba,* Tao Zheng,* Prabir Ray,* Robert J. Homer,‡§ Charles Kuhn III,¶ Richard A. Flavell,‖ and Jack A. Elias*

**Department of Internal Medicine, Section of Pulmonary and Critical Care Medicine, ‡Department of Pathology, and ‖Department of Immunobiology, Yale University School of Medicine, New Haven, Connecticut 06520; §VA-CT Health Care System, West Haven, Connecticut 06516; and ¶Department of Pathology, Brown University School of Medicine, Memorial Hospital of Rhode Island, Pawtucket, Rhode Island 02860*

Abstract

Interleukin-11 is a pleotropic cytokine produced by lung stromal cells in response to respiratory viruses, cytokines, and histamine. To further define its potential effector functions, the Clara cell 10-kD protein promoter was used to express IL-11 and the airways of the resulting transgene mice were characterized. In contrast to transgene (−) littermates, the airways of IL-11 transgene (+) animals manifest nodular peribronchiolar mononuclear cell infiltrates and impressive airways remodeling with subepithelial fibrosis. The inflammatory foci contained large numbers of B220(+) and MHC Class II(+) cells and lesser numbers of CD3(+), CD4(+), and CD8(+) cells. The fibrotic response contained increased amounts of types III and I collagen, increased numbers of α smooth muscle actin and desmin-containing cells and a spectrum of stromal elements including fibroblasts, myofibroblasts, and smooth muscle cells. Physiologic evaluation also demonstrated that 2-mo-old transgene (+) mice had increased airways resistance and non-specific airways hyperresponsiveness to methacholine when compared with their transgene (−) littermates. These studies demonstrate that the targeted expression of IL-11 in the mouse airway causes a B and T cell–predominant inflammatory response, airway remodeling with increased types III and I collagen, the local accumulation of fibroblasts, myofibroblasts, and myocytes, and obstructive physiologic dysregulation. IL-11 may play an important role in the inflammatory and fibrotic responses in viral and/or nonviral human airway disorders. (*J. Clin. Invest.* 1996. 98:2845–2853.) Key words: epithelial cell • fibrosis • cytokine • myofibroblast • collagen

Introduction

Obstructive airways disorders are a major cause of morbidity and mortality, with asthma affecting ~ 9–12 million people (1, 2), chronic obstructive pulmonary disease (COPD)[1] affecting 12–14 million people (3), and bronchiolitis and bronchiectasis affecting large numbers of people (4, 5) in the United States alone. Chronic airway inflammation and airway remodeling (defined as fibrosis, matrix alterations, and/or changes in structural or resident cells of the airway wall) are important features of these disorders (3–11). However, the pathogenetic mechanisms that generate these responses and the relationship between these responses and the physiologic dysregulation characteristic of these disorders are poorly understood.

Respiratory viruses play an important role in obstructive disorders of the human airway. Viruses are important precipitants of asthmatic exacerbations (6, 12–15) and may similarly exacerbate COPD (16). In addition, epidemiologic investigations have demonstrated important associations between infantile viral infections and the existence of asthma (12, 13, 17, 18), and pediatric infections and COPD (16, 19) in later life. These viral effects are felt to be mediated via a number of mechanisms, including the induction and modulation of local inflammation (10, 12, 20). Virus-stimulated cytokine production is increasingly understood to play a prominent role in the generation of these inflammatory abnormalities (6, 21–23). The contribution(s) that each virus-stimulated cytokine makes to the pathologic and physiologic abnormalities characteristic of viral infections in hosts with normal and obstructed airways has, however, been inadequately investigated. In addition, we know little about the mechanism(s) by which pediatric viral infections and virus-induced cytokines predispose to airways disorders in later life.

IL-11 was initially discovered as a plasmacytoma proliferation stimulating activity in supernatants from transformed marrow fibroblasts (24, 25). In accordance with this finding, most studies of IL-11 have focused on its roles in hematopoiesis (25). IL-11 has, however, been shown to have a variety of other bioactivities, including the ability to stimulate the acute phase response (25), augment the production of metalloproteinase inhibitors (26, 27), increase immunoglobulin production (25, 28), and alter neural phenotype (29). Previous studies from our laboratory demonstrated that human lung fibroblasts and epithelial cells produce IL-11 in response to cytokines (IL-1 and TGF-β_1), histamine, and viruses that have been epidemiologically associated with asthmatic exacerbations (rhinovirus, respiratory syncytial virus [RSV], and parainfluenza virus type 3, [PIV3]) (21, 30, 31). Our studies have also demonstrated that IL-11 can be found in the nasal secretions of children with viral upper respiratory tract infections and that IL-11 induces

Address correspondence to Jack A. Elias, Yale University School of Medicine, Section of Pulmonary and Critical Care Medicine, Department of Internal Medicine, 333 Cedar Street, 105 LCI, New Haven, CT 06520. Phone: 203-785-4163; FAX: 203-785-3826.

Received for publication 30 May 1996 and accepted in revised form 10 October 1996.

The Journal of Clinical Investigation
Volume 98, Number 12, December 1996, 2845–2853

1. *Abbreviations used in this paper:* AHR, airways hyperresponsiveness; BAL, bronchoalveolar lavage; CC10, clara cell 10-kD protein; COPD, chronic obstructive pulmonary disease; MCh, methacholine; PIV3, parainfluenza virus type 3; RSV, respiratory syncytial virus.

airways hyperresponsiveness (AHR) when inhaled in a transient fashion into murine lungs (23). As a result of these observations, we postulated that IL-11 plays an important role in the pathogenesis of human airway disorders, particularly those that are associated with viral infections.

In keeping with the chronic nature of disorders such as asthma, COPD, bronchiectasis, and bronchiolitis, we addressed this hypothesis by defining the respiratory tract manifestations of IL-11 when chronically present in the respiratory tract. This was done by generating and evaluating the airways of transgenic mice in which the Clara cell 10-kD protein (CC10) promoter was used to target IL-11 to the respiratory tree. These studies demonstrate that IL-11 causes impressive airway alterations with transgene (+) animals manifesting a nodular B and T cell–predominant peribronchiolar inflammatory response, bronchial remodeling with subepithelial fibrosis, and physiologic dysfunction characterized by airways obstruction and nonspecific AHR.

Methods

Production and identification of transgenic mice. To study the effector functions of IL-11 in the airway, we took advantage of the fact that the murine respiratory tract epithelium contains 50–60% clara cells (32, 33). As previously described (32), we used the promoter of the CC10 gene to target the expression of human IL-11 to airway tissues. The rat CC10 promoter was a gift of Drs. Barry Stripp and Jeffrey Whitsett (34). It was isolated as a 2.3-kb HindIII fragment and subcloned into the HindIII site of construct pKS-SV40, yielding construct pKS-CC10-SV40. pKS-SV40 had been previously prepared by inserting a 0.85-kb BglII/BamHI fragment containing SV40 intronic and polyadenylation sites into the BamHI site in construct pBluescript IIKS (Stratagene Inc., La Jolla, CA). The cDNA encoding human IL-11 was a generous gift of Dr. Paul Schendel (Genetics Institute, Cambridge, MA). It was isolated as a 1.2-kb EcoRI fragment, end filled with Klenow enzyme and subcloned into the EcoRV site in pKS-CC10-SV40 using standard techniques. All constructs were checked for correct orientation of the inserts by restriction enzyme digestion, and junction sequences were confirmed by sequencing. The resulting CC10-IL-11-SV40 construct was purified, digested with Asp 718 and BamHI to generate the CC10-IL-11-SV40 fragment (Fig. 1), separated by electrophoresis through 1% agarose, and isolated by electroelution into dialysis tubing. The DNA fragment was then purified through Elutip-D columns following the manufacturer's instructions (Schleicher and Schuell, Inc., Keene, NH) and dialyzed against injection buffer (0.5 mM Tris-HCl/25 mM EDTA, pH 7.5). Transgenic mice were prepared in (CBA × C57 BL/6) F_2 eggs using standard pronuclear injection as previously described (32, 35). The presence or absence of the transgene was evaluated in offspring animals using tail-derived DNA. This was initially done by Southern blot analysis using ^{32}P-labeled IL-11 cDNA as a probe. Similar results were obtained by PCR using 5′-CGACTGGACCGGCTGCTGC-3′ and 5′-CTAACTAGGGGGAGATAATGGCGGGGGGA-3′ as upper and lower primers, respectively. 35 cycles were performed. Each cycle was heated at 95°C for 1 min, annealed at 63°C for 1 min, and elongated at 72°C for 2 min.

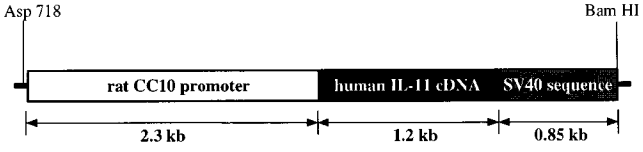

Figure 1. Schematic illustration of CC10-IL-11 construct used in the preparation of the transgenic mice described in this manuscript.

Bronchoalveolar lavage and quantification of IL-11 levels. Mice were killed via cervical dislocation, a median sternotomy was performed, blood was obtained via right heart puncture and aspiration, and serum was prepared. The trachea was then isolated via blunt dissection and small caliber tubing was inserted and secured in the airway. Three successive washes of 0.75 ml PBS with 0.1% BSA were then instilled and gently aspirated. Each bronchoalveolar lavage (BAL) aliquot was centrifuged and the supernatants were harvested and stored individually at −70°C until ready to be used. The levels of IL-11 in the BAL fluid and serum were quantitated immunologically via ELISA and biologically using the B9.11 plasmacytoma proliferation bioassay. The ELISA was performed as previously described by our laboratory (21, 30) using antibodies 11h3/15.6.1 and 11h3/19.6.1 provided by Dr. Edward Alderman (Genetics Institute). The bioassay was also performed as previously described by our laboratory (36, 37) using B9.11 cells also provided by Genetics Institute. Since both IL-6 and IL-11 can stimulate B9.11 cell proliferation, this assay was performed in the presence and absence of neutralizing antibodies against IL-11 (a gift of Dr. Alderman) and IL-6 (a gift of Dr. Pravin Sehgal, New York Medical College, Valhalla, NY) to assess the relative contribution of each of these moieties.

Northern analysis. Total cellular RNA from a variety of mouse tissues was obtained using guanidine isothiocyanate extraction and formaldehyde-agarose gel electrophoresis as previously described (21, 30). IL-11 gene expression was assessed by probing with ^{32}P-labeled IL-11 cDNA. Equality of sample loading and efficiency of transfer were assessed via ethidium bromide staining.

Histologic evaluation. Animals were killed via cervical dislocation, median stenotomies were performed, and right heart perfusion was accomplished with calcium and magnesium-free PBS to clear the intravascular space. The heart and lungs were then removed en bloc, inflated with 1 cc neutral buffered 10% formalin, fixed overnight in 10% formalin, embedded in paraffin, and sectioned and stained. Hematoxylin and eosin, and Mallory's trichrome stains were performed.

Morphometric analysis. Morphometric study was carried out on mice aged 15 d, 1 mo, and 2 mo. The thickness of the walls of small airways from the base of the columnar epithelium to the outer limit of the adventitia was measured using an eye-piece reticle. Bronchioles < 250 μm in diameter that presented a closed circular or oval profile were selected and all measurements were made at 400 magnification to the nearest whole micrometer. The wall thickness was routinely evaluated at two points on opposite sides of the short axis of the elliptical profiles and measurements were made at locations where cell borders appeared sharp to minimize tangential sectioning. 5–12 airways were measured per mouse, mean 8.4. The presence or absence of lymphoid nodules was recorded for each bronchiolar profile, whether or not it was considered appropriate for measuring wall thickness. Statistical evaluations of the morphometric results were performed by the Bonferonni multiple comparisons test using Instat software for the Macintosh.

Immunohistochemistry. Animals were killed, the vascular tree was perfused, and the heart and lungs were removed en bloc as described above. The tissues were then processed using a number of approaches. For evaluations of cell surface markers and subepithelial airway cellularity, lungs were inflated with 1 × PBS/33% (vol/vol) OCT tissue-tek compound (Miles Laboratories, Inc., Elkhart, IN) and snap frozen in OCT by submersion into 2-methylbutane cooled with dry ice. Tissue sections were cut, transferred onto silane-treated glass slides, fixed with acetone for 15 min, and stained with various antibody reagents as previously described (32). Sections were blocked with avidin-blocking kit (Vector Laboratories, Inc., Burlingame, CA) and BSA before reaction with the desired biotinylated primary antibody. The slides were then washed three times (in 0.1 M Tris buffer, pH 7.5) and the tissue sections were incubated with a prediluted streptavidin-alkaline phosphatase solution (Vector Laboratories, Inc.) for 1 h. The sections were washed and developed using Vector red staining (Vector Laboratories, Inc.) in accordance with the manufacturer's instructions. The slides were counter stained with

Meyer's hematoxylin, and then mounted with aqueous histologic mounting medium (Zymed Laboratories, Inc., So. San Francisco, CA).

For types I and III collagen immunostaining, mouse lungs were chilled in acetone containing protease inhibitors (20 mM iodoacetamide and 2 mM phenylmethyl sulfonyl fluoride) at −20°C for 16–20 h. The lungs were then chopped into ~ 2 × 5 × 6 mm^3 pieces and immersed three times in glycol methacrylate (GMA) monomer at 4°C for 6 h. The samples were then embedded in GMA according to the manufacturer's instructions (JB4 Embedding Kit; Polysciences Inc., Warrington, PA) and 2-μm sections were cut and transferred onto silane-treated glass slides. Immunohistochemical staining was undertaken as described above except that sections were treated with 1 M citric acid (pH 3.0) for 2 h before staining, and primary antibody incubation took place at 4°C overnight.

The antibodies that were employed and their sources are listed below. They included antibodies to CD3, CD4, CD8 (Gibco Laboratories, Grand Island, NY), Mac-1 (Pharmingen, San Diego, CA), B220 (Pharmingen), MHC Class II (a gift from Dr. Kim Bottomly, Yale University), type I collagen (Chemicon International, Inc., Temecula, CA), type III collagen (a gift from Dr. J. Madri, Yale University), α-smooth muscle actin (Sigma Chemical Co., St. Louis, MO), and desmin (Sigma Chemical Co.).

Electron microscopy. Fragments of lung from three age- and sex-matched littermate pairs were fixed in 3% gluteraldehyde, postfixed in osmium tetroxide, and embedded in Epox 812 (Ernest F. Fulham, Inc., Latham, NY). Tissues were then cut onto grids, stained with uranyl acetate and lead nitrate, and examined in a Philips 300 microscope (Philips Electronic Instruments, Inc., Mahwah, NJ).

Physiologic evaluation of transgenic mice. Age, sex, and weight matched littermate mice were anesthetized with pentobarbital (90 mg/kg) and tracheostomized with an 18-gauge angiocatheter. Airways resistance was then measured using a modification of the techniques described by Martin et al. (38) as previously described (32). With these techniques, the changes in the lung volumes of anesthetized and tracheostomized mice were measured plethysmographically by determining the pressure in a Plexiglass chamber using an inline microswitch pressure transducer. Flow was measured by differentiation of the volume signal and transpulmonary pressure was determined via a second Microswitch pressure transducer placed in line with the plethysmograph and animal ventilator. Resistance was then calculated using the method of Amdur and Mead (39). The resistance of the tracheostomy catheter was routinely eliminated. Baseline measurements of pulmonary resistance were obtained by ventilating the mouse in the plethysmograph at volumes of 0.4 ml at a rate of 150 breaths per minute (settings previously shown to produce normal arterial blood gases in this species) (38). Bronchial reactivity was also assessed using noncumulative methacholine challenge procedures as previously described by our laboratory (32). In this procedure, increasing concentrations of methacholine (MCh) in PBS were administered by nebulization (20 one-ml breaths) using a Devilbiss Aerosonic nebulizer (Model 5000; DeVilbiss Health Care, Somerset, PA) that produces particles 1–3 μM in diameter. Pulmonary resistance was calculated precisely 1 min later. Stepwise increases in MCh dose were then given until the pulmonary resistance, in comparison with the baseline level, had at least doubled. All animals received serial threefold increases in MCh from 1 to 100 mg/ml. The data are expressed as the PC_{100} (provocative challenge 100), the dose at which pulmonary resistance was 100% above the baseline level as calculated by linear regression analysis.

Statistical analysis. Values are expressed as means±SEM. Unless otherwise noted, group means are compared with the Student's two tailed unpaired *t* test using the StatView software for the Macintosh.

Results

Generation of transgenic mice. To generate transgenic mice in which IL-11 is overproduced in a lung-specific/selective fashion, pronuclear microinjections of the CC10-IL-11-SV40 construct were performed on two separate occasions. From these microinjections, seven animals with transgene copy numbers varying between 1 and 70 were obtained (Fig. 2). These founder animals were bred with C57 BL/6 mice and the transgene status of these offspring were similarly analyzed. This analysis demonstrated that the transgenes passed on to the off-

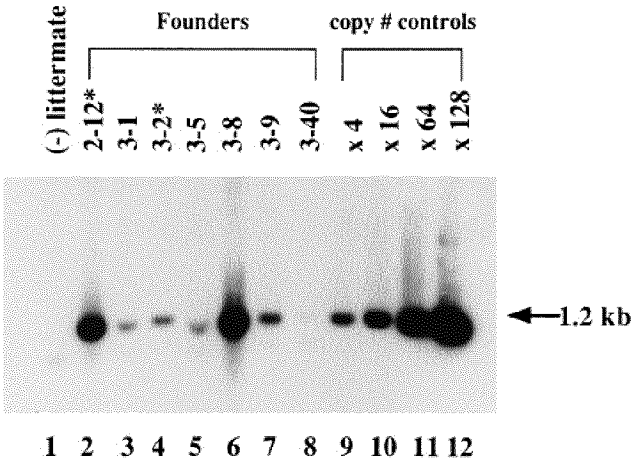

Figure 2. Southern blot analysis of CC10-IL-11 mice. Tail DNA was obtained and the presence or absence of the CC10-IL-11 construct was determined using Southern blot analysis as described in Methods. The results obtained using tail DNA from transgene (+) founder animals (lanes *2–8*) are compared with a transgene (−) littermate (lane *1*) and copy number control (lanes *9–12*).

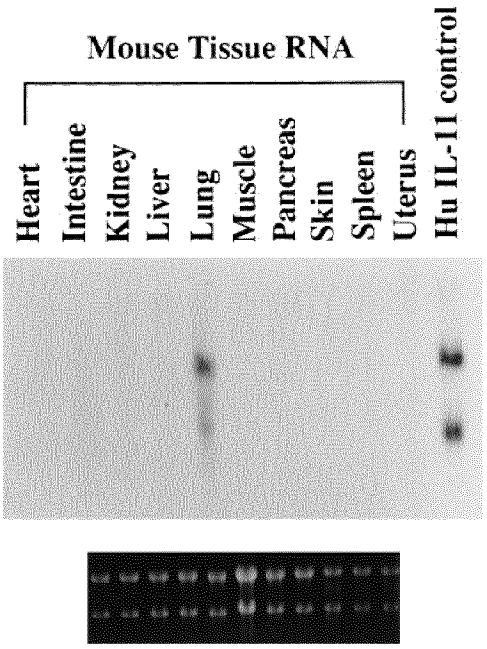

Figure 3. Northern blot analysis of IL-11 mRNA expression in mouse organs. Total cellular RNA was isolated from the noted organs of transgene (+) CC10-IL-11 mice and the levels of IL-11 mRNA characterized using Northern blot analysis as described in Methods. The IL-11 mRNA in total cellular RNA from the different tissues is compared with the IL-11 mRNA in TGF-β_1 (10 ng/ml)–stimulated human lung fibroblasts (*Hu IL-11 control*). Ethidium bromide controls are in bottom panel.

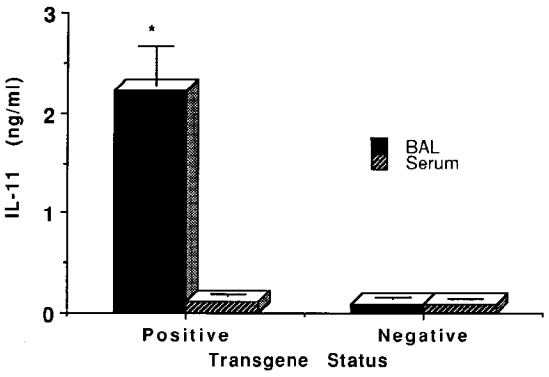

Figure 4. Levels of immunoreactive IL-11 in BAL fluid and serum of transgene (+) and (−) littermates. The noted values represent the mean±SEM of the evaluations of four separate pairs of transgene (+) and (−) littermates (*$P < 0.01$ vs. serum of transgene (+) animals and BAL and serum of transgene (−) animals; paired *t* test).

spring of these founder animals in a Mendelian fashion. Of these founders, lines 2-12 and 3-2 were chosen for more extensive analysis. Since they manifest similar pathologic, immunologic, and physiologic abnormalities, they will be discussed in a unified fashion.

Organ specificity and intensity of IL-11 gene expression and protein production. To determine if the CC10-IL-11 transgene was appropriately expressed, Northern analysis was used to compare the levels of IL-11 mRNA in the lungs and extrapulmonary organs of transgene (+) and (−) littermates. IL-11 mRNA was readily detected in the lungs of transgene (+) animals, but could not be appreciated in the lungs of transgene (−) animals (Fig. 3 and data not shown). In accordance with in vitro studies using fibroblasts and epithelial cells (21, 30), this IL-11 mRNA appeared to have one major and one minor transcript. IL-11 gene expression also appeared to be appropriately targeted to the lung since human IL-11 mRNA was not detectable in the RNA from a variety of extrapulmonary organs (Fig. 3). In all cases, IL-11 mRNA appeared to be appropriately translated since IL-11 was easily detected immunologically and biologically in the BAL fluid of the transgene (+) animals, but not in the serum of transgene (+) animals or the serum or BAL fluid of transgene (−) littermates (Fig. 4 and Table I).

Table I. IL-11 Bioactivity in BAL Fluids From Transgene (+) and (−) Animals

	[^{3}H]-Tdr incorporation‡	
Incubation conditions*	No antibody	+ Anti–IL-11
BAL (−)	3,178±3,708	1,705±166
BAL (+)	57,383±5,351	5,568±378
BAL (+)	52,960±4,717	6,189±5,507
Negative control	1,896±101	—

*BAL were performed on transgene (+) and (−) littermate F_2 progeny of IL-11 transgenic mice. ‡B9.11 plasmacytoma [^{3}H]-Tdr incorporation assessed in the presence and absence of anti–IL-11. BAL plasmacytoma-stimulating activities are compared with the proliferation ([^{3}H]-Tdr incorporation) of B9.11 cells incubated in medium alone (negative control). Values represent the mean±SEM of triplicate determinations.

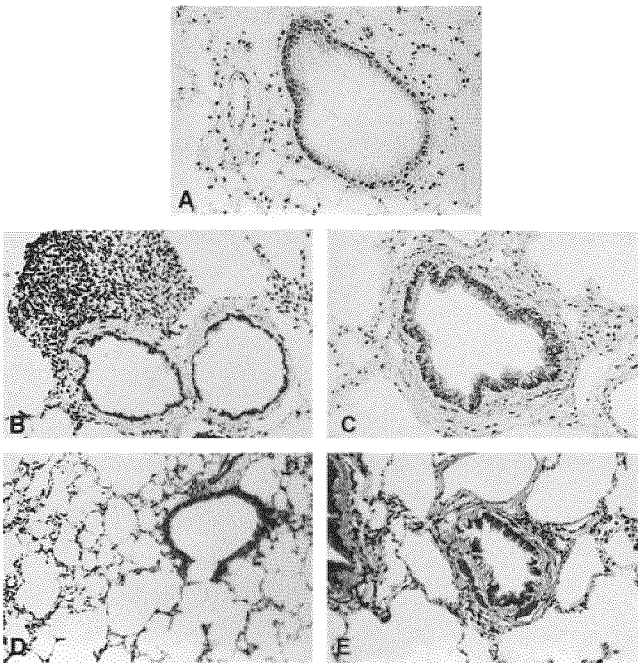

Figure 5. Histologic abnormalities in airways of CC10-IL-11 transgenic mice. The lungs of transgene (+) and (−) animals were removed, fixed, and evaluated using hematoxylin and eosin and trichrome stains. The histologic appearance of the transgene (−) mouse lung (*A*) is compared with the peribronchiolar lymphocytic infiltrates and bronchiolar thickening in the transgene (+) animals (*B* and *C*). The collagen content of the lungs of transgene (−) animals appears in green in *D*. This contrasts with the impressive subepithelial fibrosis seen in the airways of transgene (+) animals (*E*). (Original magnification 67.5×.)

Effect of IL-11 on murine airways. Progeny mice were killed at various intervals between 0.5 and 2 mo of age, and the airways of transgene (+) and (−) littermates were compared. A total of 78 age and sex matched littermate pairs were evaluated. In contrast with their transgene (−) littermates, the transgene (+) animals manifest an impressive airway phenotype composed of: (*a*) nodular collections of lymphocyte-like cells next to bronchi and bronchioles, and (*b*) airway wall thickening and remodeling (Fig. 5, *A–C*). The collections of lymphocytes were appreciated less often in the 0.5-mo-old animals, but were prominently noted in the 1- and 2-mo-old animals (data not shown). The impressive and progressive effects of IL-11 on the thickness of the airway wall were easily seen in the morphometric evaluations (Fig. 6). Insight into the cause of this thickening and remodeling was obtained from the trichrome evaluations. These stains demonstrated only small amounts of collagen in the lungs of transgene (−) animals. This contrasted with the extensive subepithelial fibrosis seen in the airways of the IL-11 transgene (+) animals (Fig. 5, *D* and *E*).

Composition of peribronchiolar nodules. The results noted above demonstrate that IL-11 overexpression in the murine airway generates nodular collections of lymphocyte-like mononuclear cells. The phenotype of these cells was, therefore, analyzed by immunohistochemistry using frozen lung sections. These studies demonstrated that the majority of the cells in these nodules were MHC Class II (+) and B220 (+) (Fig. 7). Collections of CD3(+), CD4(+), and CD8(+) cells were also noted (Fig. 6). Significant Mac-1 immunoreactivity was not

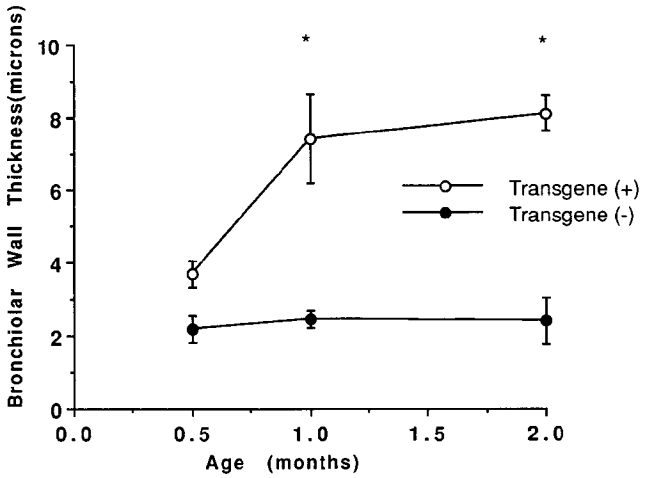

Figure 6. Morphometric analysis of airway wall thickening of CC10-IL-11 animals. The thickness of the bronchioles of 0.5-, 1-, and 2-mo-old transgene (+) and (−) littermates were measured as described in Methods. Values represent the mean±SEM of at least three pairs of animals at each time point (*$P < 0.001$ Bonferonni Multiple comparisons test).

appreciated with only a rare cell staining with this antibody (Fig. 7). None of the antibodies that were used reacted with the airways in sections of lung from transgene (−) mice, in great extent because of the lack of airway inflammation in these animals (data not shown). These observations demonstrate that these nodules are composed of large numbers of B lymphocytes and lesser numbers of CD4(+) and CD8(+) T cells.

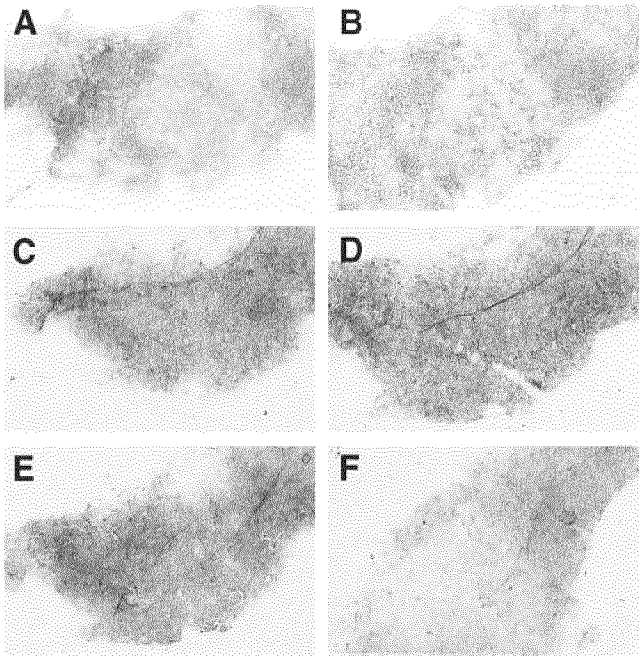

Figure 7. Immunohistochemistry of peribronchiolar nodular infiltrates. Immunohistochemical techniques were used to evaluate the cellular composition of the peribronchiolar infiltrates seen in the transgene (+) CC10-IL-11 animals. Antibodies against B220 (*A*), MHC class II (*B*), CD3 (*C*), CD4 (*D*), CD8 (*E*), and Mac-1 (*F*) were employed. (Original magnification 50×.)

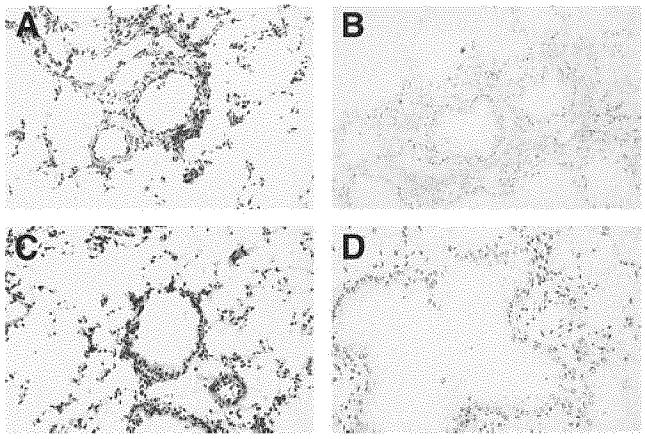

Figure 8. Immunohistochemical analysis of fibrotic response in CC10-IL-11 transgenic mice. Immunohistochemistry was used to evaluate the type I collagen in the airways of transgene (+) (*A*) and (−) (*C*) animals and the type III collagen in the airways of transgene (+) (*B*) and (−) (*D*) animals. (Original magnification 50×.)

Composition of the subepithelial fibrotic response. Studies were undertaken to determine if types I or III collagen were increased in the airways of the transgene (+) animals. These immunohistochemical evaluations demonstrated modest increases in type I collagen and impressive increases in type III collagen in transgene (+) vs. (−) animals (Fig. 8). Thus, the subepithelial fibrosis seen in CC10-IL-11 transgenic animals results, at least in part, from the increased accumulation of type III and, to a lesser extent, type I collagens.

Structural characterization of the transgenic airway. Immunohistochemistry and electron microscopy were used to further characterize the cellular and structural alterations in the airways of the CC10-IL-11 transgene (+) animals. The immunohistochemical evaluations demonstrated an increase in the

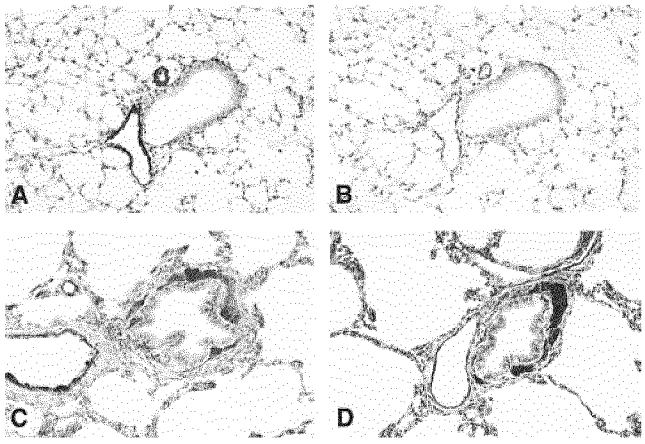

Figure 9. Immunohistochemical evaluation of subepithelial cellularity in CC10-IL-11 mice. Immunohistochemistry was used to evaluate the cellular components of the subepithelial fibrotic response in CC10-IL-11 transgene (+) and (−) animals. *A* and *C* represent the α–smooth muscle actin immunoreactivity in transgene (−) and (+) animals, respectively. *B* and *D* represent the desmin immunoreactivity in transgene (−) and (+) animals, respectively. (Original magnification 50×.)

DOCKET ALARM

Explore Litigation Insights

Docket Alarm provides insights to develop a more informed litigation strategy and the peace of mind of knowing you're on top of things.

Real-Time Litigation Alerts

Keep your litigation team up-to-date with **real-time alerts** and advanced team management tools built for the enterprise, all while greatly reducing PACER spend.

Our comprehensive service means we can handle Federal, State, and Administrative courts across the country.

Advanced Docket Research

With over 230 million records, Docket Alarm's cloud-native docket research platform finds what other services can't. Coverage includes Federal, State, plus PTAB, TTAB, ITC and NLRB decisions, all in one place.

Identify arguments that have been successful in the past with full text, pinpoint searching. Link to case law cited within any court document via Fastcase.

Analytics At Your Fingertips

Learn what happened the last time a particular judge, opposing counsel or company faced cases similar to yours.

Advanced out-of-the-box PTAB and TTAB analytics are always at your fingertips.

API

Docket Alarm offers a powerful API (application programming interface) to developers that want to integrate case filings into their apps.

LAW FIRMS
Build custom dashboards for your attorneys and clients with live data direct from the court.

Automate many repetitive legal tasks like conflict checks, document management, and marketing.

FINANCIAL INSTITUTIONS
Litigation and bankruptcy checks for companies and debtors.

E-DISCOVERY AND LEGAL VENDORS
Sync your system to PACER to automate legal marketing.